

The influence of torsion on disc herniation when combined with flexion

Samuel P. Veres · Peter A. Robertson ·
Neil D. Broom

Received: 14 September 2009/Revised: 8 February 2010/Accepted: 15 March 2010/Published online: 1 May 2010
© Springer-Verlag 2010

Abstract The role of torsion in the mechanical derangement of intervertebral discs remains largely undefined. The current study sought to investigate if torsion, when applied in combination with flexion, affects the internal failure mechanics of the disc wall when exposed to high nuclear pressure. Thirty ovine lumbar motion segments were each positioned in 2° axial rotation plus 7° flexion. Whilst maintained in this posture, the nucleus of each segment was gradually injected with a viscous radio-opaque gel, via an injection screw placed longitudinally within the inferior vertebra, until failure occurred. Segments were then inspected using micro-CT and optical microscopy in tandem. Five motion segments failed to pressurize correctly. Of the remaining 25 successfully tested motion segments, 17 suffered vertebral endplate rupture and 8 suffered disc failure. Disc failure occurred in mature motion segments significantly more often than immature segments. The most common mode of disc failure was a central posterior radial tear involving a systematic annulus–endplate–annulus failure pattern. The endplate portion of these radial tears often propagated contralateral to the direction of applied axial rotation, and, at the lateral margin, only those fibres inclined in the direction of the applied torque were affected. Apart from the 2° of applied axial rotation, the methods employed in this study replicated those used in a previously published

study. Consequently, the different outcome obtained in this study can be directly attributed to the applied axial rotation. These inter-study differences show that when combined with flexion, torsion markedly reduces the nuclear pressure required to form clinically relevant radial tears that involve cartilaginous endplate failure. Conversely, torsion appears to increase the disc wall's resistance to radial tears that do not involve cartilaginous endplate failure, effectively halving the disc wall's overall risk of rupture.

Keywords Lumbar · Intervertebral disc · Flexion · Torsion · Herniation · Microstructure

Introduction

The potential for torsion to damage intervertebral discs was first examined by Farfan [1, 2]. After axially rotating both whole motion segments and isolated discs to failure, Farfan found that torsional damage manifested as separation of the disc's peripheral lamellae and foraminal occlusion, similar to the annular changes observed during the early stages of disc degeneration. Further, Farfan et al. [2] hypothesized that repeated torsional damage may cause radial tears of the annulus, communicating from nucleus to disc periphery.

Contrary to Farfan's views, Adams and Hutton [3] subsequently argued that except for events involving severe trauma, torsion could not damage intervertebral discs. In vivo studies have shown that the range of axial rotation per lumbar motion segment is limited to 1°–2° from its neutral position [4–7]. Following the removal of motion segments' facet joints, the limiting components during axial rotation, Adams and Hutton [3] found that isolated discs were relatively mobile: they did not sustain

S. P. Veres (✉) · N. D. Broom
Department of Chemical and Materials Engineering,
University of Auckland, Level 8, Room 1.810,
20 Symonds Street, Auckland 1010, New Zealand
e-mail: s.veres@auckland.ac.nz

P. A. Robertson
Department of Orthopaedic Surgery, Auckland Hospital,
2 Park Road, Grafton, Auckland 1023, New Zealand

damage until they had been rotated through angles ranging from 10° to 20°, well above the physiologic norm.

Whilst torsion alone may not pose a threat to the structural integrity of lumbar intervertebral discs, it appears to have a marked effect when applied in conjunction with flexion. In vitro mechanical testing of motion segments has demonstrated that although the addition of a torsional moment to discs that are cyclically flexed whilst compressed does not increase the incidence of herniation, it does induce herniation in significantly fewer loading cycles [8]. Similarly, epidemiologic evidence suggests that amongst persons who lift heavy objects on a daily basis with low frequency, those who couple lifting with a twisting motion are over three times as likely to suffer a herniated lumbar disc, whilst twisting does not increase this risk for those who lift with high frequency [9].

Why the combination of flexion and torsion may act to expedite disc herniation is unknown. The combined action of flexion and torsion has been found to shift the nucleus posterolaterally in an asymmetric fashion, such that during flexion plus left axial rotation the nucleus is pushed against the right posterolateral annulus [10]. Using finite element analysis, Schmidt et al. [11] found that under this same loading combination, flexion plus left axial rotation, the fibres of the inner right posterolateral annulus experience the largest shear strain. It is possible that the combination of flexion and torsion may act to drive a herniation posterolaterally, contributing to the radial tears and herniations that occur in this region, as documented in cadaveric studies [12, 13] and clinical practice [14–16].

Recently, Veres et al. [17] explored the internal failure mechanics of lumbar intervertebral discs subjected to high nuclear pressures whilst positioned in flexion. Analysis of the ruptured discs using micro-computed tomography (micro-CT) and microscopy in tandem revealed that a radial tear of the central posterior disc wall involving both annular and endplate disruption was the most common cause of disc failure. Using this previous study's methodology as a base, the current study sought to determine if a physiologic level of torsion, when applied in combination with flexion, alters the internal failure mechanics of discs subjected to high nuclear pressures.

Methods

Ten freshly harvested ovine lumbar spines, from animals age 2–5 years, were wrapped in plastic film and stored at –20°C for no more than 3 months. In preparation for testing, the extraneous soft tissues and posterior elements were removed from each spine, as described previously [18]. Each spine was then dissected into L12, L34 and L56 motion segments by bisecting the adjacent discs. Each

bisected disc was visually inspected; no macroscopic ruptures, clefts, or areas of discoloration were found.

To ensure a consistent level of hydration during testing, each motion segment was soaked for 20 h in 0.15 M saline at 4°C. The exterior of each intervening disc was then wrapped in saline-soaked gauze covered by plastic film to impede water loss. It is important to note that, compared to the physiologic state, this process would likely result in discs being superhydrated, thereby facilitating rupture. Following the method of Schechtman et al. [19], a hollow injection screw (internal bore diameter 1.5 mm) was inserted longitudinally through the inferior vertebra of each segment so that its tip contacted the centre of the nucleus. Each motion segment's vertebrae were then potted in stainless steel rings using dental plaster, aligned so that the two rings and inferior vertebra were coaxial.

A custom-built, bench-top rig was used to position each motion segment in a combined posture of left axial rotation and flexion, which was maintained throughout the testing process. First, the superior vertebra of each segment was axially rotated 2° to the left about a fixed axis running longitudinally through the inferior vertebra and passing through the centre of the nucleus. Motion segments were then flexed 7° about a fixed axis running perpendicular to the sagittal plane of the inferior vertebra and intersecting the torsional axis in the nucleus. Both the torsion and flexion rotations were carried out gradually at approximately 0.02°/s.

To allow visual monitoring of the discs during nuclear pressurization, the saline-soaked gauze covering each disc's exterior was removed. Using a quick release coupling, each segment's embedded injection screw was connected to a manually actuated piston–cylinder device containing a viscous contrast gel, described previously [18]. A pressure transducer (model LM/2345-6, Sensotec, USA; ±0.3 MPa accuracy), mounted at the base of the injection screw, and data logger (model TC-08, PicoLog software version 5.13.4; Pico Technology, UK) were used to monitor and record the pressure of the injected gel throughout testing.

The pressure within each disc's nucleus was gradually increased in a ramp-and-hold manner, as employed previously [17, 18], by advancing the piston 0.3 mm at a rate of 0.008–0.013 mm/s and then waiting 12–14 s before the next advance. When failure of each segment occurred, marked by a focal protrusion, extrusion, and/or a sudden drop in nuclear pressure, the injection process was halted and the intradiscal pressure immediately relieved. After removing the injection screw, each motion segment's vertebrae were transected leaving approximately 5 mm of bone attached to both ends of the disc. These trimmed segments were immediately wrapped in plastic film and frozen at –20°C.

Using a micro-CT scanner (model 1172, SkyScan, Belgium) operating at 100 kV/100 μ A, each trimmed motion segment was imaged at a resolution of 34.6 μ m, allowing a three-dimensional assessment of the injected contrast gel entrapped within. The resulting data set for each segment was processed into axial and sagittal image sets using NRecon and DataViewer software (version 1.5.0.2 & 1.3.2, SkyScan), and subsequently flattened into maximal intensity projection (MIP) images using CTAn software (version 1.7.0.5, SkyScan).

Following micro-CT, each segment was fixed in 10% formalin and decalcified in 10% formic acid. The posterior portion of each segment was then processed into approximately 100, 30 μ m thick, oblique radial bone-disc-bone cryosections using a freezing-sledging microtome, as illustrated previously [18]. Cryosections were wet-mounted and examined unstained using oblique illumination microscopy.

Statistics were computed using SPSS software (version 12.0.1). Mean failure pressures were compared using a one-way ANOVA with post hoc Scheffé's test. Categorical group-outcome correlations were tested for significance using Fisher's exact test.

Results

A total of 30 motion segments, dissected from 10 spines, were tested. Peak rates of pressurization ranged from 0.03 to 0.11 MPa/s. Five motion segments exhibited abnormal pressure–time responses and very low disc:vertebra gel content ratios, indicative of gel leakage at the inferior vertebra/injection screw interface. These five segments, which had failed to pressurize correctly, were excluded from the results.

Following analysis using micro-CT and microscopy, each motion segment was classified as suffering either vertebral or disc failure. Motion segments that suffered catastrophic failure of a vertebral endplate, leading to gel and/or nuclear extrusion into a vertebral body, were classified as vertebral failures. The remaining motion segments, which suffered predominantly soft-tissue failure, were classified as disc failures. Of the 25 successfully tested motion segments, 17 suffered vertebral failure and 8 disc failure.

The skeletal maturity of each motion segment was assessed using posterior cryosections by microscopically examining the vertebral growth plates superior and inferior to the intervening disc. Each motion segment's growth plates were recorded as fused, partially fused or unfused. When the fused and partially fused categories were combined, a significant correlation between motion segment maturity and failure mode was found: mature segments (those with fused or partially fused growth plates) were significantly more likely to suffer disc failure than immature segments ($p = 0.01$; Table 1).

Table 1 A significant correlation was observed between motion segment maturity, as indicated by vertebral growth plate morphology, and mode of failure ($p = 0.01$)

	Vertebral failure	Disc failure	Disc failure fraction (%)
Fused and partially fused	5	7	58
Unfused	12	1	8

In all 25 successfully tested motion segments, axial micro-CT MIP images showed that from the point of injection near the centre of the nucleus, the contrast gel spread laterally filling the nuclear lobes. Penetration of the annulus by the contrast gel occurred exclusively at the central posterior location, with the exception of a single disc where a small volume of contrast gel entered the anterior annulus.

Vertebral failures

Seventeen motion segments suffered vertebral failure. Rupture of the inferior vertebral endplate adjacent to the centre of the nucleus was the most common cause of vertebral failure, occurring in 11 segments (note that the inferior vertebral endplate, described here in relation to the disc, is the cranial endplate of the motion segment's caudal vertebra). In six segments, the point of failure was readily distinguishable from the hole left by the injection screw (dashed line in Fig. 1), most often lying to the posterior (* in Fig. 1). Whilst the point of vertebral endplate failure in the remaining five segments could not be accurately distinguished from the hole left by the injection screw, the segments displayed normal pressure–time responses and micro-CT scans, and thus could not be discounted as technical failures. Centrally located ruptures of the superior vertebral endplate were considerably less frequent, occurring in only four segments. The remaining two segments suffered vertebral endplate failure adjacent to the right mediolateral aspect of the nucleus, one inferiorly and the other superiorly.

Microscopy revealed that the injected contrast gel had breached the inner posterior annulus in 8 of the 17 motion segments that suffered vertebral endplate failure, but had failed to penetrate the discs radially beyond this point. Apart from the location of catastrophic vertebral endplate failure, no additional sites of endplate disruption were found in any of the 17 motion segments.

Disc failures

Eight motion segments suffered disc failure. Microscopic analysis of posterior cryosections revealed that each disc

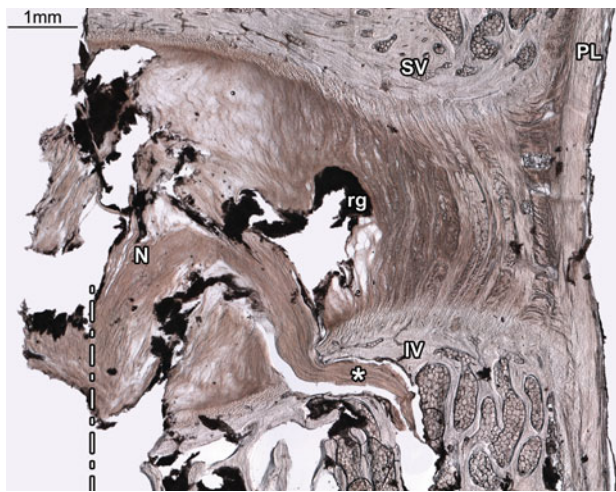


Fig. 1 Rupture of the inferior vertebral endplate was the most common mode of failure amongst tested motion segments. In this disc (2-L56) the inferior vertebral endplate has ruptured near the nucleus/annulus transition zone, allowing nuclear material to enter the inferior vertebral body (asterisks). The dashed line marks the centre of the hole through which the injection screw was inserted. The injected contrast gel (rg) has reached the inner posterior annulus, but has failed to penetrate the disc radially beyond this point, leaving the mid and outer portions of the disc intact. N nucleus, SV superior vertebra, IV inferior vertebra, PL posterior longitudinal ligament

had suffered one of three distinct modes of failure: *diffuse rupture* of the posterior annulus (Fig. 2C), *radial annular-endplate tear* of the central posterior disc wall (Fig. 3C), or *radial mid-axial tear* of the central posterior annulus (Fig. 6B). Morphologic details for each of the eight cases

of disc failure are listed in Table 2. The incidence of each mode of disc failure per total discs tested is listed in Table 3.

Diffuse ruptures

Two discs suffered diffuse rupture of the posterior annulus. Each contained a large volume of contrast gel within the posterior annulus, which had formed sequential circumferential tears by flowing within the fibre bundles of the inner and mid-annular lamellae (* in Fig. 2A, C). The circumferential tears were connected by short radial tears (arrows in Fig. 2C) that were circumferentially distributed (a single tissue section was unlikely to contain a radial tear). In both discs, contrast gel had pooled behind the posterior longitudinal ligament ('v' in Fig. 2C), causing severe disruption to the outer annular lamellae before extruding mediolaterally at the left margin of the posterior longitudinal ligament. A small tear within the superior cartilaginous endplate, adjacent to the inner posterior annulus, existed within disc 8-L56 ('ep' in Fig. 2C). No other form of endplate disruption was observed in these two discs.

Radial tears

The remaining six discs contained very little contrast gel within the posterior annulus, indicating that failure had occurred suddenly rather than in a progressive fashion as occurred in the two previously described cases of diffuse

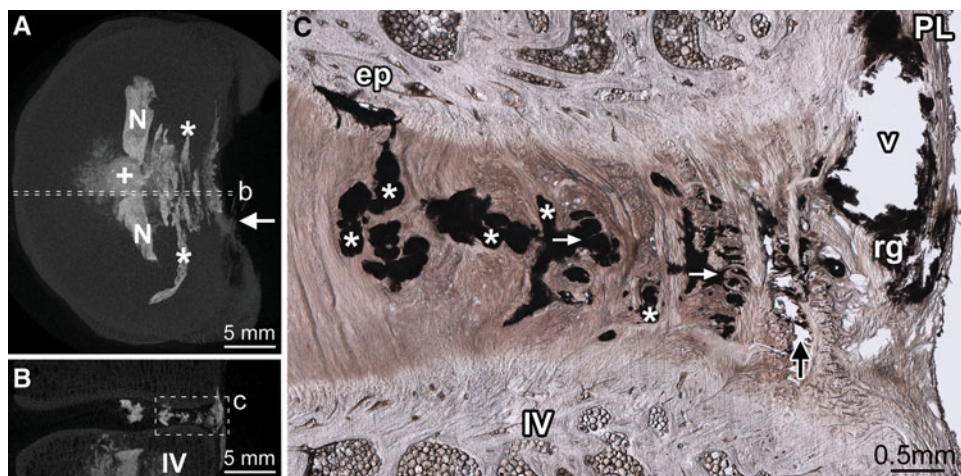


Fig. 2 Diffuse rupture of the posterior annulus. Disc 8-L56 is shown. Dashed lines in the axial (A) and sagittal (B) micro-CT MIP images show the location of the micrograph (C). From the point of injection (+ in A), contrast gel has spread laterally filling the nuclear lobes (N in A). After penetrating the inner posterior annulus, the gel has spread circumferentially, flowing within the inner and mid-annular lamellae (* in A and C). Two short radial tears, connecting some of the circumferential tears, are visible in C (white arrows). Upon reaching

the outer annulus, gel has flowed primarily between lamellae (black arrow in C). In both discs that suffered diffuse ruptures, the contrast gel failed to rupture the posterior longitudinal ligament (PL in C), leaving a large void (v in C) outlined in residual gel (rg in C) as it tracked circumferentially to its point of extrusion at the ligament's left lateral margin (white arrow in A). IV inferior vertebra, ep tear of the cartilaginous endplate

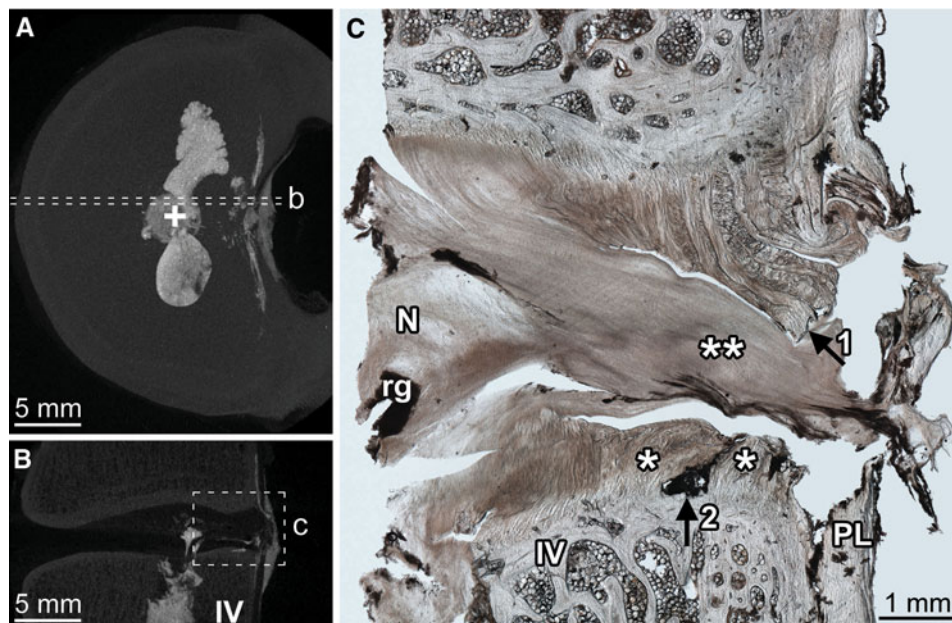


Fig. 3 Radial annular-endplate tear of the central posterior disc wall was the most frequent cause of disc failure. Disc 3-L34 is shown. The axial (A) and sagittal (B) micro-CT MIP images show the location of the micrograph (C). Radial annular-endplate tears were characterized by two regions of annular failure (* in C), separated by an endplate tear adjacent to the mid-annulus (arrow 2 in C). In this disc, the tear

failure (for example, Figs. 3A, 4A or 5A each show less posterior contrast than Fig. 2A). At the point of failure, five of the six discs extruded gel from the central posterior annulus, which was accompanied by nuclear material in two discs. The other disc (disc 5-L56) extruded gel from the right mediolateral aspect of the posterior annulus. Microscopy confirmed that each of the six discs had suffered a radial tear extending through the central posterior disc wall from nucleus to disc periphery.

Radial annular-endplate tears: In five of the six discs that suffered radial tears, the tears followed the same general morphologic pattern: failure of the inner annulus, followed by an endplate tear adjacent to the mid-annulus, followed by failure of the outer annulus (Fig. 3C). The endplate tear occurred superiorly in one disc and inferiorly in the four others. In the central posterior region, where the radial tears communicated from nucleus to disc periphery, endplate tears always occurred between the vertebral and cartilaginous endplates (i.e. at the cartilaginous/vertebral endplate junction), and extended a radial length of approximately 1 mm. Circumferentially, the endplate portion of the radial tears extended farther than the annular portion (i.e. the endplate portion of the tears extended over a greater lateral distance). In two discs, the endplate tear extended 3 mm to either side of the disc's sagittal plane, whilst in three discs the endplate tear extended only towards the right (again by approximately 3 mm). Details of each disc's endplate tear are listed in Table 2.

contains a large volume of nuclear material (** in C), which has severed the posterior longitudinal ligament forming a transligamentous nuclear extrusion. Prior to rupture, the separated regions marked by arrows 1 and 2 in C would have been connected. N nucleus, rg residual gel, IV inferior vertebra, PL posterior longitudinal ligament

In three of the five discs that suffered radial annular-endplate tears, the morphology of the endplate tear varied with circumferential location. Whilst the endplate tear was radially continuous at the central posterior location (Fig. 4D), mediolaterally only those fibres inclined in the direction of the applied torque had been affected (Fig. 4E). Further, whereas the central posterior portion of these endplate tears always occurred at the cartilaginous/vertebral endplate junction (Fig. 4D), mediolaterally the lamellae failed at the annulus/cartilaginous endplate junction (Fig. 5C).

Radial mid-axial tear: Sample 8-L23 was the only disc with unfused endplates to suffer disc failure, and the only disc to suffer a radial tear through the entire thickness of the central posterior annulus in the mid-axial plane (Fig. 6B). Interestingly, disc 8-L23 also suffered an endplate tear located adjacent to the mid-annulus at the cartilaginous/vertebral endplate junction (arrow in Fig. 6A). However, unlike the discs that suffered radial annular-endplate tears, this endplate tear was located beyond the right lateral margin of the radial mid-axial tear, and therefore appeared not to have directly contributed to the disc's catastrophic failure.

Discussion

The current study has used the technique of nuclear pressurization, employed previously [17–20], to mechanically

Table 2 Mode of failure and endplate tear morphology for motion segments that suffered disc failure

Segment (spine-disc)	Growth plate status	Failure pressure (MPa)	Mode of failure	Endplate tear						
				Torn endplate	Radial location ^a	Circumferential		Vertical location		
						Location	Span (mm)	IML	C	rML
3-L56	F	7.1	Diff	–	–	–	–	–	–	–
8-L56	F	11.4	Diff	sup	inner	C → rML	2.9	–	E	E
8-L12	U	10.5	MA ^b	inf	mid	rML	1.5	–	–	E/V
7-L12	P	9.0	AE	sup	mid	C → rML	4.1	–	E/V	+ E/V
3-L34	P	8.0	AE ^b	inf	mid	C → rML	2.9	–	E/V	E/V
5-L56	F	7.4	AE	inf	mid	C → rML	2.5	–	E/V	+ A/E
5-L34	F	4.2	AE	inf	mid	IML → rML	5.6	E/V	E/V	E/V
5-L12	P	5.6	AE	inf	mid	IML → rML	5.9	E/V	E/V	+ A/E

F fused, P partially fused, U unfused, Diff diffuse rupture, MA radial mid-axial tear, AE radial annular-endplate tear, sup superior, inf inferior, C central posterior, IML left mediolateral posterior, rML right mediolateral posterior, E within the cartilaginous endplate, E/V between the cartilaginous and vertebral endplates, A/E between the annulus and cartilaginous endplate, + = only fibres inclined in the direction of the applied torque were ruptured

^a As defined in Fig. 7

^b Transligamentous nuclear extrusion

Table 3 The variation in disc failure mode with motion segment posture during nuclear pressurization

	7° flexion ^a	7° flexion + 2° torsion	10° flexion ^a
Incidence per total discs tested			
Diffuse ruptures	18% (3/17)	8% (2/25)	6% (1/17)
Radial mid-axial tears	24% (4/17)	4% (1/25)	0% (0/17)
Radial annular-endplate tears	24% (4/17)	20% (5/25)	35% (6/17)
Mean failure pressure ± SD (MPa)			
Total disc failures	11.2 ± 2.5*	7.9 ± 2.4*	9.8 ± 2.6
Radial annular-endplate tears	9.4 ± 1.4	6.8 ± 1.9	9.2 ± 2.3

*Indicates a significant difference ($p = 0.03$; one-way ANOVA, Scheffé’s post hoc)

^a Data from Veres et al. [17]

disrupt intact intervertebral discs positioned in a combined posture of 7° flexion plus 2° axial rotation. Micro-CT and optical microscopy have subsequently been used in tandem to investigate how this posture affects the internal failure mechanics of discs.

With the exception of the 2° of applied axial rotation, the methods used to mechanically disrupt motion segments in this study replicated, as exactly as possible, those previously used to disrupt motion segments that were pressurized whilst flexed 7° [17]. Given that the ovine tissue used in these two studies was similarly distributed according to skeletal maturity, the differences in failure response of the motion segments between these two inter-study groups can be directly attributed to the applied axial rotation.

Together, the results of this study and those from the 7° flexion group tested previously [17] show that when

combined with flexion, axial rotation (1) reduces the occurrence of radial tears confined solely to the annulus and (2) facilitates the formation of radial tears that involve an endplate tear adjacent to the mid-annulus.

Of the total motion segments successfully tested in the current study, 32% suffered disc failure. Amongst the motion segments previously pressurized whilst flexed 7° [17], this proportion was 65%. In both studies, the same three modes of disc failure were identified: diffuse rupture, radial mid-axial tears, and radial annular-endplate tears. The observed decrease in the proportion of disc failures with the addition of 2° of axial rotation occurred primarily as the result of a decrease in diffuse ruptures and radial mid-axial tears: failure modes that generally only incorporate annular disruption (Table 3).

Previously, it was found that increasing the flexion angle of discs subjected to nuclear pressurization from 7° to 10°

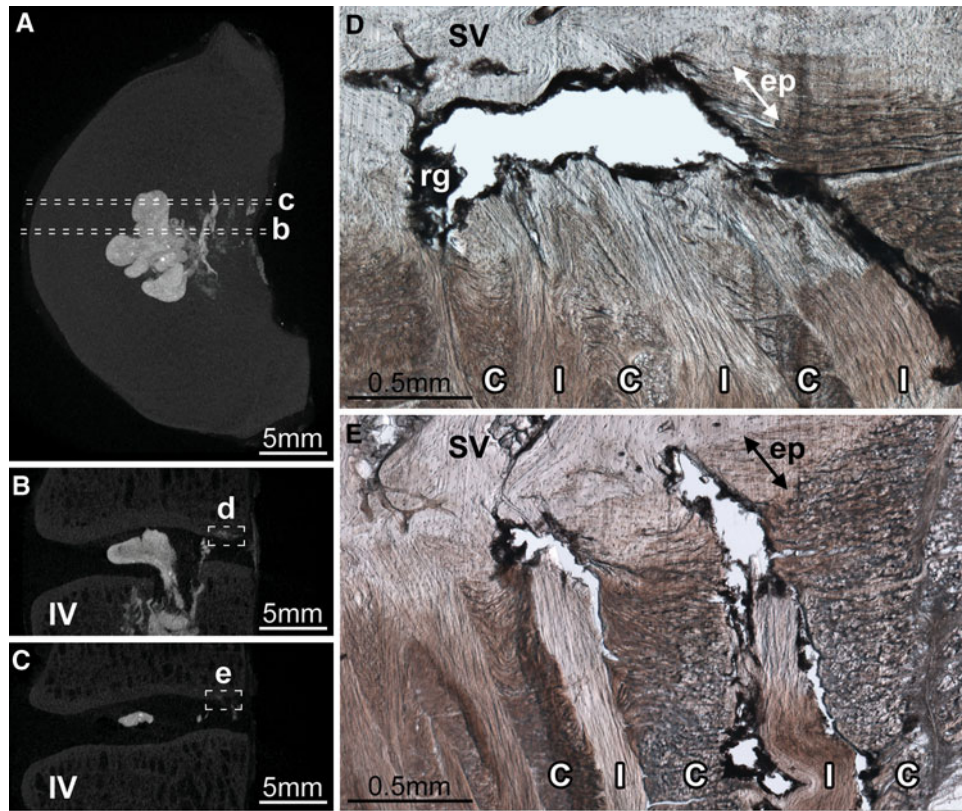
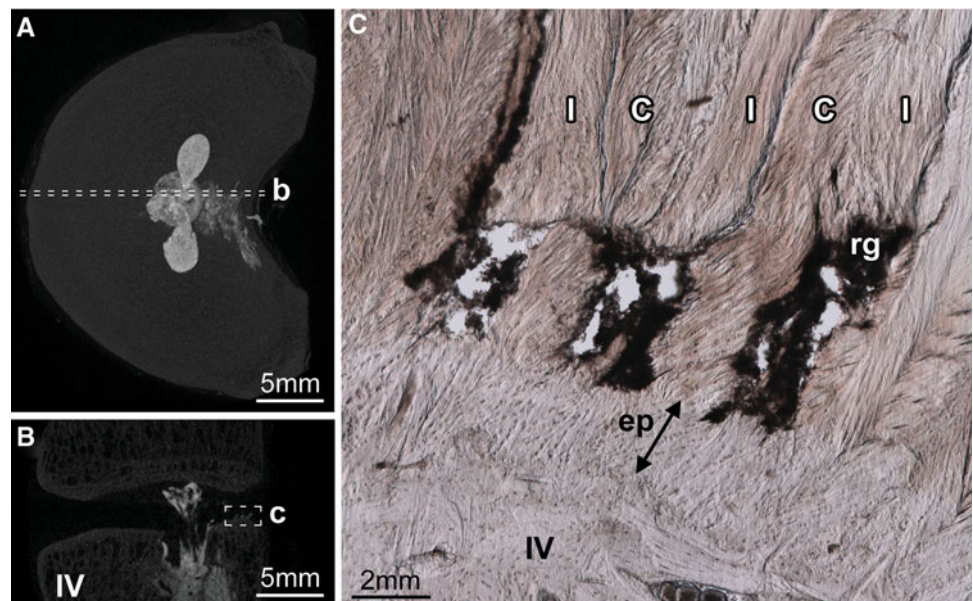


Fig. 4 The variation in endplate tear morphology with circumferential location in radial annular-endplate tears. Disc 7-L12 is shown. The axial (A) and sagittal (B, C) micro-CT MIP images show the location of the micrographs (D, E). The endplate portion of the radial annular-endplate tears spanned between 2.5 and 5.9 mm circumferentially, most often extending to the right from the discs' midline (Table 2). At the central posterior location tears always occurred at the cartilaginous/vertebral endplate junction and extended a radial

distance of approximately 1 mm, disrupting the anchorage of both in-plane (I) and cross-sectioned (C) lamellae (D). The right mediolateral aspect of the endplate tears were often morphologically distinct; only fibres inclined in the direction of the applied axial rotation were affected (I vs. C in E). IV inferior vertebra, SV superior vertebra, rg residual gel. Arrows marked 'ep' indicate the thickness of the cartilaginous endplate

Fig. 5 The axial (A) and sagittal (B) micro-CT MIP images show the location of the micrograph (C). Whilst the endplate portion of radial annular-endplate tears usually occurred at the cartilaginous/vertebral endplate junction, in two discs the right mediolateral portion of the endplate tear occurred at the annulus/endplate junction (disc 5-L12 is shown). In both discs, only fibres inclined in the direction of the applied axial rotation were ruptured, in this case those of the in-plane lamellae (I), but not the cross-sectioned lamellae (C). IV inferior vertebra, rg residual gel. The arrow marked 'ep' indicates the thickness of the cartilaginous endplate



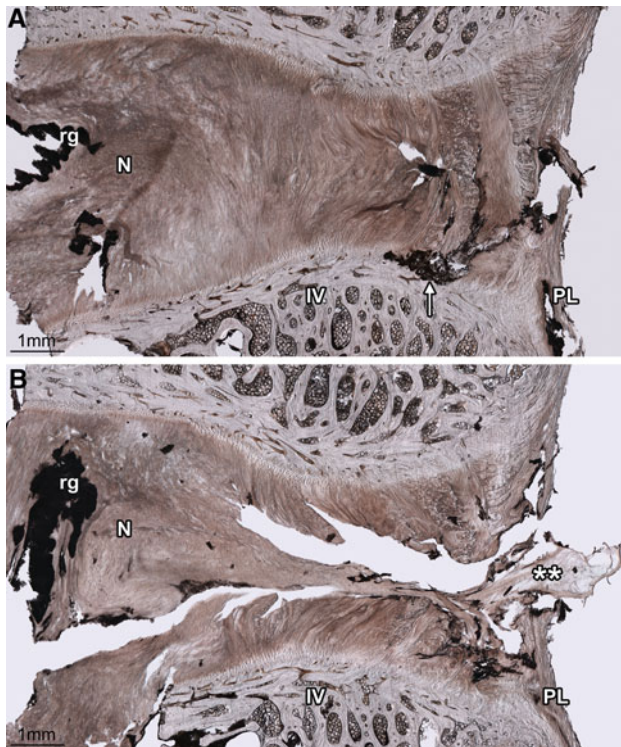


Fig. 6 The unique case of disc 8-L12, shown here, highlights that whilst torsion tended to direct endplate tears contralaterally, the central posterior portion of the disc wall was most vulnerable to radial tearing. The two cryosections shown lie approximately 1.5 mm apart in the same plane. **A** This right mediolateral cryosection shows an endplate tear adjacent to the mid-annulus (*arrow*). **B** This central posterior cryosection shows that nuclear material (***) has bisected the annulus, forming a radial mid-axial tear resulting in a transligamentous nuclear extrusion. No form of endplate disruption is present in this cryosection. *N* nucleus, *IV* inferior vertebra, *PL* posterior longitudinal ligament, *rg* residual gel

resulted in an increased incidence of radial annular-endplate tears [17]. These tears are clinically significant: they always occur in the central posterior location and detach a portion of cartilaginous endplate adjacent to the mid-annulus (as defined in Fig. 7), most often inferiorly. Clinically, approximately 50% of disc herniation routes are documented as radially traversing the central posterior disc wall [16, 21], most often inferiorly [21], and are often associated with endplate disruption [22, 23]. Compared to the 7° flexion group tested previously [17], and in contrast to an additional 3° of flexion [17], the 2° of superimposed axial rotation used in the current study did not lead to an increased incidence of radial annular-endplate tears. It did, however, markedly reduce the pressure at which these tears occurred (Table 3).

Compared to the flexed state, only Drake et al. [8] have previously used in vitro testing to assess whether combining flexion with torsion alters the disruption mechanics of discs. In their study, porcine cervical motion segments

were cyclically flexed and extended whilst compressed. During cyclic loading, one group of specimens was subjected to a static axial torque; the other was not. Whilst an equal number of discs in both groups herniated (7/9), axial torque induced herniation in fewer loading cycles. Epidemiologically, Kelsey et al. [9] studied the relationship between occupational lifting and twisting, and suffering a herniated lumbar disc. Their results indicate that when lifting, simultaneous twisting only increases the risk of disc herniation amongst persons who perform the task with low to moderate frequency and not high frequency.

The results of our current study, together with those of Drake et al. [8] and Kelsey et al. [9], suggest that given a population of discs, some will be susceptible to herniation when exposed to compression plus flexion. Axial rotation, if combined with compression and flexion, will not increase the proportion of susceptible discs, but will, however, facilitate the herniation process amongst those discs at risk.

Because radial tears involving endplate failure constituted approximately 60% of the disc failures in the current study, the above interpretation should more appropriately specify: ‘Axial rotation, if combined with compression and flexion, will [...] facilitate the herniation process amongst those discs at risk of a *radial annular-endplate tear*’. This specification is important; compared to the 7° flexion group tested previously [17], the addition of axial rotation halved the overall incidence of disc failure by markedly reducing the number of failures that involved only the annulus (Table 3). Consequently, the fact that torsion decreased the mean disc failure pressure in the current study likely results from the endplate’s inability to cope with the mechanical effects of torsion.

It is intuitive that the addition of axial rotation to a flexed disc would increase the posterior cartilaginous/vertebral endplate junction’s susceptibility to failure; annular fibres inclined in the direction of rotation would experience higher magnitudes of axial (normal) strain. Similarly, one might assume that a posture of 10° flexion would place this junction at greater risk of failure than 7° flexion plus 2° axial rotation. Given that the flexion and torsion axes intersected near the centre of the nucleus in this experiment, 10° flexion would produce larger peak axial strains in the posterior annulus. However, the mean nuclear pressure required to cause radial annular-endplate tears in the current study was nearly 30% lower than that required when discs are flexed 10° (Table 3). Whilst 7° flexion plus 2° axial rotation would impose lower peak axial strains on posterior annular fibres than 10° flexion, it would generate higher magnitudes of shear stress at the endplate/vertebra junction.

If the endplate/vertebra junction is sensitive to shear stress, this negative torsional effect would be further

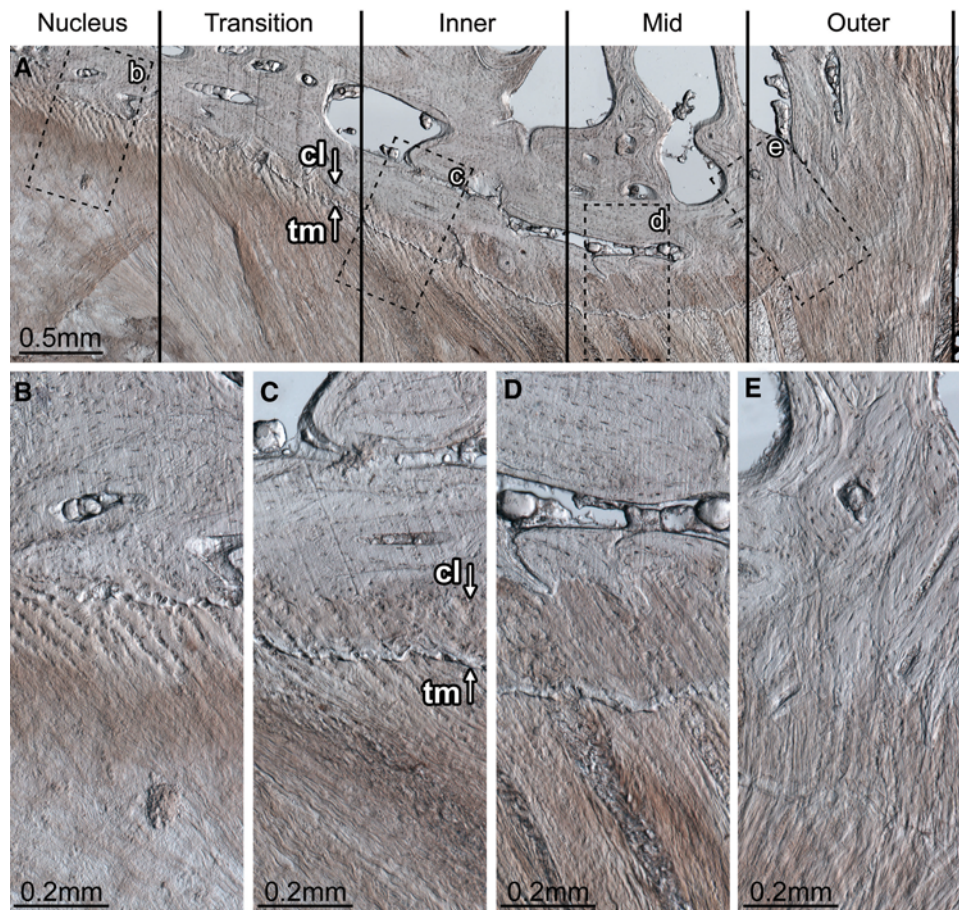


Fig. 7 Endplate morphology and disruption susceptibility. The disc wall can be divided into three morphologically distinct zones: inner, mid and outer. Between the nucleus and inner zone exists the transition zone. The transition zone contains fibres that have a well-defined superior–inferior orientation, but are not organized into distinct lamellae. *Inner zone* (c): the inner zone begins at the first well-defined lamella. Whilst no calcification of the cartilaginous endplate is present adjacent to the nucleus (B), adjacent to the transition and inner zones both calcified and uncalcified cartilaginous endplate exist (C). The boundary between the calcified and uncalcified cartilage, the tidemark, is indicated by arrow *tm* in C. The boundary between the calcified cartilage and the vertebral endplate, the cement line, is indicated by arrow *cl* in C. The ratio of calcified to uncalcified cartilage increases with increasing radial distance away

compounded by uneven load sharing amongst lamellae. Tensile testing has shown that annular lamellae function in a non-linear stress–strain fashion; they become stiffer as they are stretched [24–26]. Consequently, when a disc is axially rotated, every second lamella effectively becomes stiffer than its two neighbours. This creates an uneven load-sharing situation when the nucleus is pressurized: the stiffer, more highly strained lamellae will support most of the applied load. Thus, compared to the flexed state, the addition of torsion may be detrimental to the disc by forcing half of the annular lamellae to support well over half of the applied nuclear pressure, therefore increasing peak stresses at the cartilaginous/vertebral endplate

from the nucleus. *Mid-zone* (d): the cartilaginous endplate is fully calcified. The cement line is well defined. There appears to be little to no connection between the annular fibres penetrating the cartilaginous endplate and the vertebral endplate. It is the endplate in this zone that is always implicated in radial annular-endplate tears and appears to be the most prone to mechanical disruption (Figs. 3C, 4D). *Outer zone* (e): the cartilaginous endplate is fully calcified. The cement line is less prominent. Annular fibres penetrating the cartilaginous endplate appear to integrate with the vertebral endplate forming a robust disc/vertebra connection. The tissue section shown is from the mediolateral posterior aspect of a ewe's L56 disc (vertebral growth plates unfused). Note that the posterior longitudinal ligament has been removed; if present it would exist to the right of the outer zone

junction and causing localized failure adjacent to the mid-annulus as shown in Figs. 4E and 5C.

The natural history of intervertebral discs is well documented. As the disc ages, the nucleus progressively loses glycosaminoglycans, leading to dehydration [27, 28] and reduced hydrostatic functionality [29]. Whilst the nuclei of ovine discs, like that of Grade II human discs [30], is whitish, cohesive and resilient (far from a freely flowing substance), it seems unlikely that nuclear extrusion, as shown in Figs. 3C and 6B, would occur after a certain threshold level of nuclear dehydration is reached. This supposition is consistent with the fact that the risk of disc herniation diminishes markedly after the age of 50 years

[31]. Similarly, with age the cartilaginous endplates become increasingly calcified [32], which would, presumably, increase both the stiffness and brittleness of the endplate/vertebra junction.

Clinically, persons of age 40–50 years have the greatest risk of suffering a herniated lumbar disc [22, 31]. Approximately, 45% of the motion segments tested with fused or partially fused growth plates suffered radial annular-endplate tears in both the current study and our previous study of flexed discs [17]. Similarly, Adams and Hutton [33] found that approximately 65% of the motion segments from persons aged 39–51 years suffered nuclear extrusion when compressed whilst positioned in hyperflexion. The discs belonging to these susceptible subsets are clearly morphologically distinct, in some currently undefined way, from the remainder of their cohorts. It may be that in these susceptible discs the nucleus is sufficiently hydrated to flow under pressure, whilst endplate calcification has increased the stiffness of the cartilaginous/vertebral endplate junction to a point where its ultimate strength is surpassed during maximal, but normal, *in vivo* strains.

Several *in vitro* mechanical studies have previously reported the creation of posterolateral herniations [33–35]. The combination of flexion and torsion has been reported to shift the nucleus posterolaterally [10], and subject the inner posterolateral region of the annulus to the largest shear strain [11]. In the current study, a tendency for posterior endplate tears to propagate circumferentially from the central posterior location, contralateral to the direction of applied axial rotation, was noted. This finding may be due to the fact that the annular fibres medial to the pedicles and inclined in the direction of applied axial rotation are shorter contralaterally than ipsilaterally [36] and would thus be strained more highly during torsion. Despite this tendency for endplate tears to propagate contralaterally, radial tears communicating from the nucleus to the disc periphery formed centrally, consistent with the finite element modelling prediction made by Lu et al. [37]. The posterolateral disc wall appears to be very robust compared to the posterior when discs are subjected to pure flexion in the sagittal plane, as in the current study. The creation of posterolateral radial tears likely requires anterolateral bending, as demonstrated by Aultman et al. [38].

Two points should be noted regarding posterolateral herniations. First, posterolateral herniations, a term used widely in *in vitro* studies, correspond to intra or extraforaminal herniations clinically [39–41]. Such herniations are far less common than central posterior or mediolateral posterior herniations [14, 16, 21]. Second, a posterolateral protrusion or extrusion does not necessitate a posterolateral radial tear. During discography, it is not uncommon to reveal a centrally located radial tear that deviates

circumferentially at its peripheral terminus [21, 42, 43]. Such tears have been reported as a common finding during the transverse sectioning of cadaveric lumbar discs [12, 44]. Previous observations indicate that nuclear material may readily move circumferentially within the outer posterior annulus [17], which may possess weak interlamellar cohesion [18], and is prone to circumferential tearing [45]. A portion of the foraminal or intraforaminal herniations observed clinically may well connect to the nucleus via a radial tear of the central posterior disc wall.

Adams and Hutton [3, 33] have suggested that torsion is unlikely to play a role in the mechanical disruption of lumbar intervertebral discs. Whilst it may be unlikely that torsion can disrupt discs when applied as the sole rotation, the results of the current study clearly show that 2° of axial rotation when applied in combination with flexion markedly reduces the disc wall's ability to withstand high nuclear pressure. Further, flexion has been shown to increase interfacet spacing [46], thereby allowing the lumbar spine an increased range of motion in axial rotation [47–49]. Thus, if a lumbar disc can be rotated beyond the normal 2° limit whilst the spine is flexed, the negative effects of torsion demonstrated in the current study have the potential to be amplified *in vivo*.

Acknowledgment The authors are grateful for the award of grants in support of this research from Medtronic Australasia, The New Zealand Orthopaedic Association Wishbone Trust, Education New Zealand and the University of Auckland.

Conflict of interest statement Funds in support of this research were received from: Medtronic, The NZOA Wishbone Trust, The University of Auckland, and Education New Zealand.

References

1. Farfan HF (1969) Effects of torsion on the intervertebral joints. *Can J Surg* 12:336–341
2. Farfan HF, Cossette JW, Robertson GH, Wells RV, Kraus H (1970) The effects of torsion on the lumbar intervertebral joints: the role of torsion in the production of disc degeneration. *J Bone Joint Surg Am* 52:468–497
3. Adams MA, Hutton WC (1981) The relevance of torsion to the mechanical derangement of the lumbar spine. *Spine* 6:241–248
4. Gunzburg R, Hutton W, Fraser R (1991) Axial rotation of the lumbar spine and the effect of flexion. An *in vitro* and *in vivo* biomechanical study. *Spine* 16:22–28
5. Ochia RS, Inoue N, Renner SM, Lorenz EP, Lim TH, Andersson GB, An HS (2006) Three-dimensional *in vivo* measurement of lumbar spine segmental motion. *Spine* 31:2073–2078
6. Pearcy M, Portek I, Shepherd J (1984) Three-dimensional X-ray analysis of normal movement in the lumbar spine. *Spine* 9:294–297
7. Plamondon A, Gagnon M, Maurais G (1988) Application of a stereoradiographic method for the study of intervertebral motion. *Spine* 13:1027–1032
8. Drake JD, Aultman CD, McGill SM, Callaghan JP (2005) The influence of static axial torque in combined loading on

- intervertebral joint failure mechanics using a porcine model. *Clin Biomech* (Bristol, Avon) 20:1038–1045
9. Kelsey JL, Githens PB, White AA 3rd, Holford TR, Walter SD, O'Connor T, Ostfeld AM, Weil U, Southwick WO, Calogero JA (1984) An epidemiologic study of lifting and twisting on the job and risk for acute prolapsed lumbar intervertebral disc. *J Orthop Res* 2:61–66
 10. Fazey PJ, Song S, Monsas S, Johansson L, Haukalid T, Price RI, Singer KP (2006) An MRI investigation of intervertebral disc deformation in response to torsion. *Clin Biomech* (Bristol, Avon) 21:538–542
 11. Schmidt H, Kettler A, Heuer F, Simon U, Claes L, Wilke HJ (2007) Intradiscal pressure, shear strain, and fiber strain in the intervertebral disc under combined loading. *Spine* 32:748–755
 12. Lindblom K (1944) Protrusions of disks and nerve compression in the lumbar region. *Acta Radiol* 25:195–212
 13. Hirsch C, Schajowicz F (1952) Studies on structural changes in the lumbar annulus fibrosus. *Acta Orthop Scand* 22:184–231
 14. Ebeling U, Reulen HJ (1992) Are there typical localisations of lumbar disc herniations? A prospective study. *Acta Neurochir* (Wien) 117:143–148
 15. Jackson RP, Becker GJ, Jacobs RR, Montesano PX, Cooper BR, McManus GE (1989) The neuroradiographic diagnosis of lumbar herniated nucleus pulposus: I. A comparison of computed tomography (CT), myelography, CT-myelography, discography, and CT-discography. *Spine* 14:1356–1361
 16. Maezawa S, Muro T (1992) Pain provocation at lumbar discography as analyzed by computed tomography/discography. *Spine* 17:1309–1315
 17. Veres SP, Robertson PA, Broom ND (2009) The morphology of acute disc herniation: a clinically relevant model defining the role of flexion. *Spine* 34:2288–2296
 18. Veres SP, Robertson PA, Broom ND (2008) ISSLS prize winner: Microstructure and mechanical disruption of the lumbar disc annulus: part II: how the annulus fails under hydrostatic pressure. *Spine* 33:2711–2720
 19. Schechtman H, Robertson PA, Broom ND (2006) Failure strength of the bovine caudal disc under internal hydrostatic pressure. *J Biomech* 39:1401–1409
 20. Pezowicz CA, Schechtman H, Robertson PA, Broom ND (2006) Mechanisms of annular failure resulting from excessive intradiscal pressure: a microstructural–micromechanical investigation. *Spine* 31:2891–2903
 21. Ninomiya M, Muro T (1992) Pathoanatomy of lumbar disc herniation as demonstrated by computed tomography/discography. *Spine* 17:1316–1322
 22. Moore RJ, Vernon-Roberts B, Fraser RD, Osti OL, Schembri M (1996) The origin and fate of herniated lumbar intervertebral disc tissue. *Spine* 21:2149–2155
 23. Schmid G, Witteler A, Willburger R, Kuhnen C, Jergas M, Koester O (2004) Lumbar disk herniation: correlation of histologic findings with marrow signal intensity changes in vertebral endplates at MR imaging. *Radiology* 231:352–358
 24. Bass EC, Ashford FA, Segal MR, Lotz JC (2004) Biaxial testing of human annulus fibrosus and its implications for a constitutive formulation. *Ann Biomed Eng* 32:1231–1242
 25. Holzappel GA, Schulze-Bauer CA, Feigl G, Regitnig P (2005) Single lamellar mechanics of the human lumbar annulus fibrosus. *Biomech Model Mechanobiol* 3:125–140
 26. Skaggs DL, Weidenbaum M, Iatridis JC, Ratcliffe A, Mow VC (1994) Regional variation in tensile properties and biochemical composition of the human lumbar annulus fibrosus. *Spine* 19:1310–1319
 27. Antoniou J, Steffen T, Nelson F, Winterbottom N, Hollander AP, Poole RA, Aebi M, Alini M (1996) The human lumbar intervertebral disc: evidence for changes in the biosynthesis and denaturation of the extracellular matrix with growth, maturation, ageing, and degeneration. *J Clin Invest* 98:996–1003
 28. Urban JP, McMullin JF (1988) Swelling pressure of the lumbar intervertebral discs: influence of age, spinal level, composition, and degeneration. *Spine* 13:179–187
 29. Adams MA, McNally DS, Dolan P (1996) 'Stress' distributions inside intervertebral discs. The effects of age and degeneration. *J Bone Joint Surg Br* 78:965–972
 30. Thompson JP, Pearce RH, Schechter MT, Adams ME, Tsang IK, Bishop PB (1990) Preliminary evaluation of a scheme for grading the gross morphology of the human intervertebral disc. *Spine* 15:411–415
 31. Heliovaara M, Knekt P, Aromaa A (1987) Incidence and risk factors of herniated lumbar intervertebral disc or sciatica leading to hospitalization. *J Chronic Dis* 40:251–258
 32. Bernick S, Cailliet R (1982) Vertebral end-plate changes with aging of human vertebrae. *Spine* 7:97–102
 33. Adams MA, Hutton WC (1982) Prolapsed intervertebral disc. A hyperflexion injury 1981 Volvo Award in Basic Science. *Spine* 7:184–191
 34. Adams MA, Hutton WC (1985) Gradual disc prolapse. *Spine* 10:524–531
 35. Gordon SJ, Yang KH, Mayer PJ, Mace AH Jr, Kish VL, Radin EL (1991) Mechanism of disc rupture. A preliminary report. *Spine* 16:450–456
 36. Marchand F, Ahmed AM (1990) Investigation of the laminate structure of lumbar disc annulus fibrosus. *Spine* 15:402–410
 37. Lu YM, Hutton WC, Gharpuray VM (1996) Do bending, twisting, and diurnal fluid changes in the disc affect the propensity to prolapse? A viscoelastic finite element model. *Spine* 21:2570–2579
 38. Aultman CD, Scannell J, McGill SM (2005) The direction of progressive herniation in porcine spine motion segments is influenced by the orientation of the bending axis. *Clin Biomech* (Bristol, Avon) 20:126–129
 39. Costello RF, Beall DP (2007) Nomenclature and standard reporting terminology of intervertebral disk herniation. *Magn Reson Imaging Clin N Am* 15:167–174
 40. Fardon DF, Milette PC (2001) Nomenclature and classification of lumbar disc pathology. Recommendations of the Combined task Forces of the North American Spine Society, American Society of Spine Radiology, and American Society of Neuroradiology. *Spine* 26:E93–E113
 41. Knop-Jergas BM, Zucherman JF, Hsu KY, DeLong B (1996) Anatomic position of a herniated nucleus pulposus predicts the outcome of lumbar discectomy. *J Spinal Disord* 9:246–250
 42. Aprill C, Bogduk N (1992) High-intensity zone: a diagnostic sign of painful lumbar disc on magnetic resonance imaging. *Br J Radiol* 65:361–369
 43. Ohnmeiss DD, Vanharanta H, Ekholm J (1999) Relation between pain location and disc pathology: a study of pain drawings and CT/discography. *Clin J Pain* 15:210–217
 44. Hirsch C, Schajowicz F (1953) Studies on structural changes in the lumbar annulus fibrosus. *Acta Orthop Scand* 22:184–231
 45. Vernon-Roberts B, Moore RJ, Fraser RD (2007) The natural history of age-related disc degeneration: the pathology and sequelae of tears. *Spine* 32:2797–2804
 46. Drake JD, Dobson H, Callaghan JP (2008) The influence of posture and loading on interfacet spacing: an investigation using magnetic resonance imaging on porcine spinal units. *Spine* 33:E728–E734
 47. Drake JD, Callaghan JP (2008) Do flexion/extension postures affect the in vivo passive lumbar spine response to applied axial twist moments? *Clin Biomech* (Bristol, Avon) 23:510–519
 48. Hindle RJ, Pearcy MJ (1989) Rotational mobility of the human back in forward flexion. *J Biomed Eng* 11:219–223
 49. Pearcy MJ (1993) Twisting mobility of the human back in flexed postures. *Spine* 18:114–119